The Influence of a Cable on the Voltage Distribution in Transformer Windings

G. Hoogendorp, M. Popov, L. van der Sluis

Abstract—**Voltage distribution in transformer windings is influenced by the presence of a cable due to reflections of voltage and current waves at an interconnection point with the transformer. Cable resonance frequencies also influence the behavior of the cable-transformer combination. In this paper, reflection coefficients are calculated at the interconnection point of the transformer and the cable. Computations of the inter-turn voltage distribution will be performed by making use of the Hybrid model.**

Keywords: **Hybrid model, reflection, voltage distribution**

I. INTRODUCTION

THe connection of a cable to a transformer terminal forms a very common part in every power system. The cable presence affects the behavior of a cable-transformer combination considerably, especially in case of very fast transients caused by, for example, switching or lightning [1]. At high frequencies, the cable can play an important role because of its frequency-dependent impedance. Because of the different cable and transformer resonance frequencies [2], the generated voltage waveforms for different circuit topologies are different and difficult to determine. Moreover, long cables have the ability of self attenuation and distortion effect. When a steep surge propagates along the cable and reaches the transformer terminal, reflections and refractions occur at the junction between the cable and transformer. This is caused by the different surge impedances of the cable and transformer. A voltage or a current wave propagating along the cable sees the transformer surge impedance as a load connected to the receiving end of the cable.

Steep voltage surges contain high frequency oscillations, which result in increasing the voltage amplitude at the transformer terminal due to reflection. Furthermore, the refracted surge propagates inside the winding and stress the transformer insulation with its steepness and amplitude. This is the reason for premature aging of transformer insulation.

The present work deals with the analysis of the influence of a cable when it is connected to the transformer primary

winding.

An explicit comparison will be done for a case with and without a cable connection. The studied cable has a length of 100m. In this work, the Hybrid model will be used for modeling the transformer primary winding. The cable will be modeled as a single-conductor transmission line using high frequency measurements.

The calculation will be performed by dividing the frequency range into discrete steps. For each frequency step, the surge impedances and the propagation constants need to be calculated. The system of equations is based on equating the voltages at the end of a transformer winding section and at the beginning of next winding section.

The surge impedance of the cable will be calculated by taking into account the series impedance and the shunt admittance of the cable. By making use of the cable and transformer winding surge impedance, the reflection coefficient at the transformer terminal can be calculated. For extracting the time-domain voltage waveforms the modified Fourier Transform is applied. Furthermore, the inter-turn and inter-layer voltage distribution in transformer winding will be calculated and the effect of the cable on these voltages will be analyzed.

II. METHODOLOGY

The model of the transformer primary winding is based on the modified Telegrapher's equations described by:

$$\frac{\partial \mathbf{V_t}}{\partial x} = -\mathbf{L}\left(\frac{\partial \mathbf{I_t}}{\partial t}\right)$$

$$\frac{\partial \mathbf{I_t}}{\partial x} = -\mathbf{C}\left(\frac{\partial \mathbf{V_t}}{\partial t}\right) + Co[1]\frac{\partial Eo}{\partial t} \qquad (1)$$

In these equations, $\mathbf{V_t}$ and $\mathbf{I_t}$ represent the voltage and current vectors, $\mathbf{L}$ is the inductance matrix and $\mathbf{C}$ the capacitance matrix. The Hybrid method makes use of a combination of single-transmission line model (STLM) and multiconductor transmission line model (MTLM) [3], [4], [5]. Firstly, the STLM model computes the voltages in the winding sections. Thereafter, by using these voltages, the MTLM model is applied to compute voltages of each turn. The equations for STLM and MTLT are applied in matrix form and the expressions for the surge impedance and the propagation constant are included in the appendix. For each frequency step, the surge impedance and the propagation constant have to be evaluated. The frequency range observed in this study is from zero up to 100 MHz. Taking into account that the

voltage at the end of the turn will be equal to that at the beginning of the next turn, the unknown vectors $\mathbf{A_t}$ en $\mathbf{B_t}$ containing constants can be found by computing the inverse matrix. Finally, results are transformed back to time domain using the Modified Inverse Fourier Transform [6], [7]. The calculation process is performed by applying Matlab. The algorithm of the Hybrid Model is depicted in figure 1.
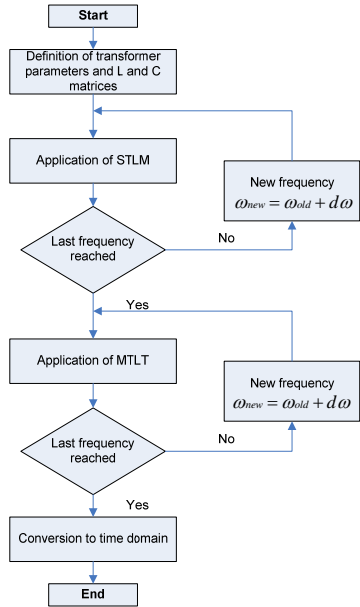
Figure 1. Description of Hybrid Model.

III. TRANSFORMER AND CABLE DATA

The transformer used for this study is a 15 kVA single phase layer-type distribution transformer. The voltage ratio is 6600V/69V and the primary winding consists of 15 layers. Every layer has 200 turns. The dimensions are given in table 1 and the studied transformer in figure 2.

TABLE I
DATA TEST TRANSFORMER

Inner radius of HV winding	73.3 mm
External radius of HV winding	97.4 mm
Inner radius of the LV winding	51 mm
External radius of LV winding	67.8 mm
Wire diameter	1.16 mm
Double wire insulation	0.09 mm
Distance between layers	0.182 mm
Coil's height	250mm
Top / bottom distance from the core	10 mm
Dielectric Permittivity of oil	2.3
Dielectric Permittivity of wire insulation	4

Figure 2. Test transformer under construction.

The Hybrid model has been verified for this transformer and successfully used for the calculation of the inter-turn voltage distributions in the primary windings. There is a good agreement between computed and the measured voltages [3]. The validity of the results obtained in this work, is primarily based on these comparisons and the computed surge impedance of the cable.

The XLPE distribution cable used in this study is modeled by its parameters, based on both geometric data and material properties [8]. Cable dielectric parameters and dimensions are given in tables 2 and 3 respectively.

TABLE 2
DIELECTRIC PARAMETERS

Parameter	Inner	Outer	Outer-outer
τ_1 (s)	1×10^{-6}	1×10^{-7}	5×10^{-8}
τ_2 (s)	4×10^{-9}	4×10^{-9}	3×10^{-8}
A_1	500	215	800
A_2	360	170	1000
α_1	0.3	0.3	0.3
α_2	0.3	0.3	0.3
σ_{dc} (mS/m)	6	5.5	800

TABLE 3
CABLE DIMENSIONS

Nominal voltage	10 kV
Length (m)	100
Inner conductor diam. (mm)	17.1
Inner semicon (mm)	1
Insulation XLPE (mm)	3.4
Outer semicon (mm)	0.5
Outer-outer semicon (mm)	0.5
Copper wire shield (mm)	1
Outer sheath (mm)	69

Using these data, the cable series impedance and shunt admittances for each semi-conducting layer can be calculated [3]. The total series impedance is equal to:

$$Z_{total} = \frac{1}{2\pi r_1}\sqrt{\frac{j\omega\mu_o}{\sigma_1}} + \frac{j\omega\mu_o}{2\pi}\ln\left(\frac{r_6}{r_1}\right) + \frac{1}{2\pi r_6}\sqrt{\frac{j\omega\mu_o}{\sigma_6}} \qquad (2)$$

The admittance for semi-conducting layer uses a complex

permittivity:

$$Y_k = j\omega \frac{2\pi\varepsilon_0\varepsilon_k}{\ln\left(\dfrac{r_k}{r_{k-1}}\right)} \qquad (3)$$

In this equation, ε_k is the complex permittivity:

$$\varepsilon(\omega) = \varepsilon'(\omega) - j\varepsilon''(\omega) \qquad (4)$$

High frequency measurements have been performed [8] to determine the material properties of the cable. The results of these measurements can be fitted using two Cole-Cole functions and a low frequency term. Based on the cable admittance and impedance, the propagation constant can be calculated:

$$\Gamma(\omega) = \sqrt{Y_{total}Z_{total}} = \alpha + j\beta \qquad (5)$$

This function is found by taking into account that the voltage at the sending end is the same as the applied voltage. When the cable length would be infinite, the voltage at the receiving end is equal to zero. By applying these boundary conditions, the propagation function is determined as:

$$H_{cable}(j\omega) = \frac{V(x, j\omega)}{G(j\omega)} = e^{-\Gamma(\omega)x} \qquad (6)$$

which also denotes the transfer function of the cable. During the computation for every frequency step, equations (2) to (6) are solved.

IV. COMPUTATION RESULTS WITHOUT CABLE

The inter-turn voltage distribution is calculated when a step function is applied directly to the transformer terminal. This situation corresponds to a fast front transient voltage as a result of, for instance, a lightning stroke. The inter-turn voltage distribution for the first layer of the transformer is shown in figure 3.
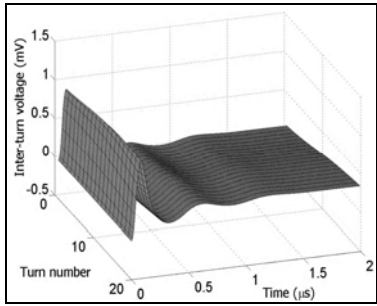
Figure 3. Inter-turn voltages in the first transformer layer with step excitation.

It can be noted that the peak inter-turn voltage is about 1 mV and the response is almost damped within 2 μs. The response for a sinusoidal excitation with amplitude of 1 V is also computed. High frequency sinusoidal excitation can represent oscillations in the system reaching the transformer terminal, after switching actions take place in the power system. The frequency of this excitation is 1.6 MHz. In figure 4, this response is plotted for the first part of the first layer. The observed peak inter-turn voltage is about 1.5 mV.
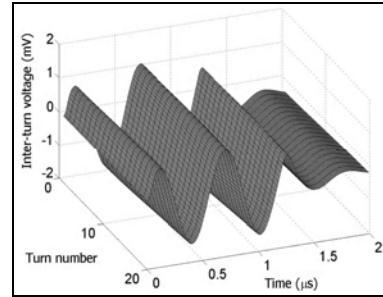
Figure 4. Inter-turn voltages in the first transformer layer with sinusoidal excitation.

In figure 5, the impulse responses are plotted for three inter-layers of the primary transformer winding. Different peaks in these responses are clearly observable for frequencies up to 10 MHz. For high frequencies, reflections take place at the junction points caused by the different surge impedances at the winding sections.
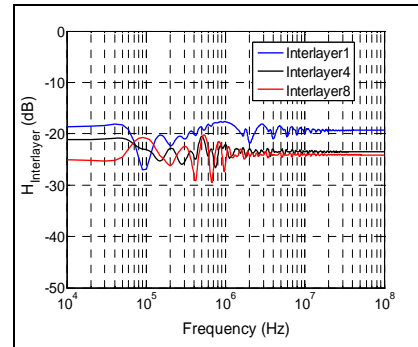
Figure 5. Inter-layer impulse response in frequency domain.

In figure 6, the impulse response for the inter-turn voltage is plotted for three inter-turns in the first winding section of the primary winding, up to 100 MHz. This plot is obtained in the same way as for the inter-layer impulse responses.
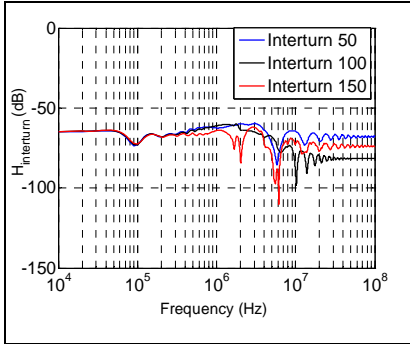
Figure 6. Inter-turn impulse response in frequency domain.

V. COMPUTATION RESULTS WITH CABLE

When a cable is connected to the transformer terminal, travelling waves experience a surge impedance mismatch at the junction point. For every frequency step, reflection can be calculated based on the cables and the transformer surge impedances. The frequency dependent reflection coefficient for the voltage wave is calculated by:

$$r = \frac{Z_{i(1)} - Z_{cable}}{Z_{i(1)} + Z_{cable}} \tag{7}$$

In this equation, $Z_{i(1)}$ and Z_{cable} are the surge impedance of the first transformer winding section and the cable respectively. Figure 7 shows the surge impedance of the first transformer layer. The surge impedance of the cable used in this study can be determined as explained in [9] and it is about 14 Ohm. The same value is found when using the Y and Z matrix of the cable based on data discussed in section III.

For lower frequencies, surge impedance of transformer winding is high compared to that of the cable, which implies that the amplitude of the reflected voltage wave is almost equal to the incident wave. In figure 8, the reflection coefficient is shown as a function of the frequency up to 100 MHz.
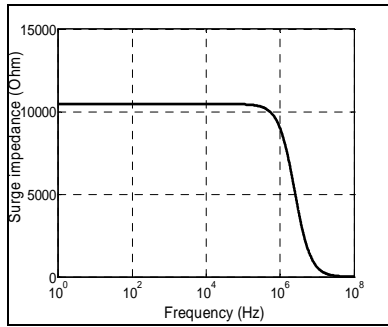
Figure 7. Surge impedance of first transformer layer.

The resulting voltage at the interconnection point is the sum of the incident and reflected voltage. The wavelength of voltage and current waves observed in transient studies is relatively short. Like all frequency dependent parameters of the transformer, the surge impedance is computed up to 100 MHz

using frequency steps. By applying equation (7), the reflection coefficient is equal to 1 for relatively low frequencies. This leads to voltage doubling at the transformer terminal. For high frequencies, the surge impedances are closer to each other. When both surge impedances are equal, the reflection coefficient becomes equal to zero and no reflections will occur at the transformer terminal.
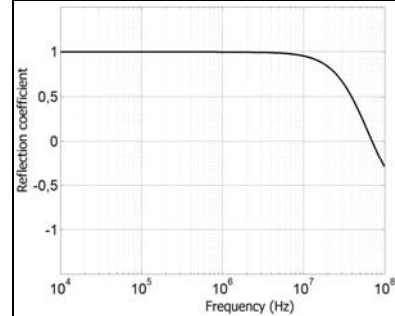
Figure 8. Reflection coefficient at cable-transformer junction.

The voltage at the receiving cable end is the same as the voltage at the transformer terminal. When the reflection is taken into account, this voltage is equal to:

$$V_r(x, j\omega) = G(j\omega)(1 + r)e^{-\Gamma(\omega)x} \tag{8}$$

For the computation, the same step function was applied to the cable sending end. In figure 9, the calculated inter-turn voltage distribution is shown for the first transformer winding section. As it can be expected from cables propagation data, the delay is about 0,6 μs. From this plot, it is clear that the peak inter-turn voltage is higher compared to the situation without a cable connected to the transformer. An ideal step voltage has an infinite steepness and thus consists of many high frequency components.

The applied input in this study is an approximated step voltage, meaning that the steepness is high but not infinite. A step function applied to a cable-transformer combination may represent the energization of a cable-transformer combination.
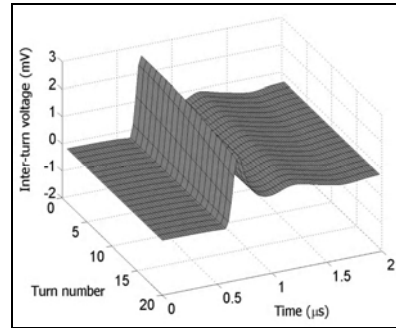
Figure 9 Inter-turn voltages with cable and step excitation.

In figure 10, the inter-turn response is depicted when a

sinusoidal voltage of 1.6 MHz is applied to the cable sending end.
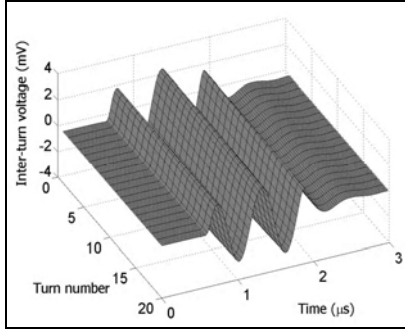
Figure 10. Inter-turn voltages with cable and sinusoidal excitation.

It can be seen that the peak inter-turn voltage is about 3 mV, which is approximately twice as high as the voltage without a cable applied between the transformer and the circuit breaker. For both situations, the responses are rapidly damped, because of the attenuation of transformer winding. Impulse responses can be obtained for both inter-layer and inter-turn voltages in a similar way as for the situation without a cable. In figure 11, the impulse responses are plotted for the same inter-layers.
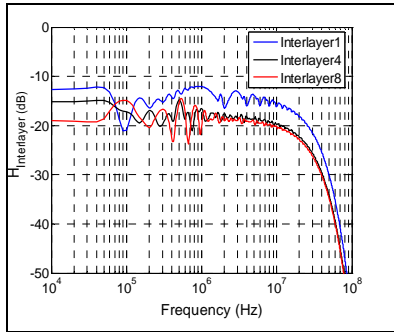
Figure 11. Impulse responses for inter-layers with cable.

It can be seen that for low frequencies, the response is about 6 dB higher than that without a cable, shown in figure 5. This means that a voltage doubling is caused by reflections as discussed earlier. In figure 12, the impulse responses of the inter-turns are plotted for the case with a cable.
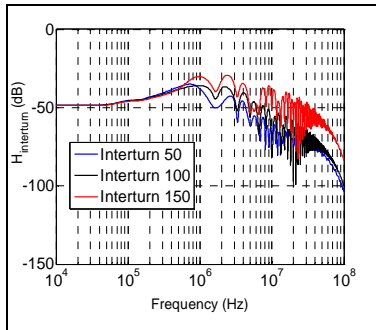
Figure 12. Impulse responses for inter-turns with cable.

VI. CONCLUSIONS

In this paper, the inter-turn voltage computation is performed for a single phase layer-type distribution transformer by applying the Hybrid Model. Two situations are distinguished. Firstly, inter-turn voltages are computed when the transformer terminal is excited by a step function. Inter-turn voltages for the first layer in time and frequency domain were considered. Secondly, the Hybrid Model is applied to compute inter-turn voltages when a distribution cable is connected to the transformer terminal. In this situation, a surge impedance mismatch exists at the transformer-cable junction. This leads to reflections of the travelling voltage and current waves at the point where transformer is connected to the cable. For lower frequencies, differences in the surge impedances of the cable and the transformer winding are large, resulting in doubling of the voltage at transformer terminal. The impulse response of both situations differs clearly for high frequencies. Likewise the inter-layer impulse responses, the inter-turn impulse responses also show a decreasing line for high frequencies.

VII. APPENDIX

The solutions of (1) for the voltages and currents in frequency domain for STLM are:

$$V_i(x) = k_i E_o + A_i \exp(-\Gamma(\omega)x) + B_i \exp(\Gamma(\omega)x)$$

$$I_i(x) = \frac{1}{z_i}\left(A_i \exp(-\Gamma(\omega)x) - B_i \exp(\Gamma(\omega)x)\right)$$

In matrix form:

$$\begin{bmatrix} \mathbf{AU(j\omega)} & \mathbf{BU(j\omega)} \\ \mathbf{AI(j\omega)} & \mathbf{BI(j\omega)} \end{bmatrix} \begin{bmatrix} \mathbf{A(j\omega)} \\ \mathbf{B(j\omega)} \end{bmatrix} = \begin{bmatrix} \mathbf{RU(j\omega)} \\ \mathbf{RI(j\omega)} \end{bmatrix}$$

The solutions of (1) for the voltages and currents in frequency domain for MTLM are:

$$V_t(x) = k_i E_o + A_t \exp(-\Gamma(\omega)x) + B_t \exp(\Gamma(\omega)x)$$

$$I_t(x) = v_s[\mathbf{C}]\left(A_t \exp(-\Gamma(\omega)x) - B_t \exp(\Gamma(\omega)x)\right)$$

In matrix form:

$$\begin{bmatrix} \mathbf{MA(j\omega)} & \mathbf{MB(j\omega)} \\ \mathbf{MC(j\omega)} & \mathbf{MD(j\omega)} \end{bmatrix} \begin{bmatrix} \mathbf{A_t(j\omega)} \\ \mathbf{B_t(j\omega)} \end{bmatrix} = \begin{bmatrix} \mathbf{UA(j\omega)} \\ \mathbf{UB(j\omega)} \end{bmatrix}$$

In these solutions, surge impedance and propagation constant [2], [3] are respectively:

$$z_i = \frac{1}{v_s\left(C_o + C_1 + K\left(1 - \cos\left(\frac{\omega a}{v_s}\right)\right)\right)}$$

$$\Gamma = \frac{1}{v_s d}\sqrt{\frac{\omega}{2\sigma\mu}} + \frac{\omega\tan\delta}{2v_s} + \frac{j\omega}{v_s}$$

Transformation to the time domain [4], [9]:

$$V(t) = \frac{2\exp(bt)}{\pi}\int_0^\Omega \frac{\sin\left(\dfrac{\pi\omega}{\Omega}\right)}{\dfrac{\pi\omega}{\Omega}}\operatorname{Re}(V(j\omega))\cos(\omega t)d\omega$$

VIII. REFERENCES

[1] T. Craenenbroek, J. De Ceuster, J. P. Marly, H. De Herdt, B. Brouwers, and D. Van Dommelen, "Experimental and numerical analysis of fast transient phenomena in distribution transformers," *in IEEE Power Eng. Soc. Winter Meeting, Singapore,* Jan. 2000.

[2] G. Paap, A. Alkema, and L. van der Sluis, "Overvoltages in power transformers caused by no-load switching," *IEEE Trans. Power Delivery*, vol. 10, pp. 301–307, Jan. 1995.

[3] G. Hoogendorp, M. Popov, L. van der Sluis "Computations on Inter-turn voltages in Transformer Windins with Interconnected Distribution Cable" *International Conference on Power Systems Transients Kyoto Japan,* June 2009

[4] M. Popov, L. van der Sluis, G.C. Paap, H. de Herdt "Computation of Very Fast Transient Overvoltages in Transformer Windings," *IEEE Trans. Power Delivery*, vol. 18, pp. 1268-1274, Oct. 2003.

[5] Y. Shibuya, S.Fujita, N. Hosokawa "Analysis of very fast transient overvoltage in transformer winding" *IEE Proc. -Gener. Transm. Distrib.*, vol. 144, pp. 462-468, Sept. 1997.

[6] J.P. Bickford J.P., N. Mullineux, J.R. Reed: "Computation of Power System Transients", *IEE, Peter Peregrinus Ltd., 1976, ISBN 0901223859.*

[7] K. Cornick, B. Filliat, C. Kieny, and W. Müller, "Distribution of very fast transient overvoltages in transformer winding," *in CIGRE, Paris, France,* 1992, paper 12-204

[8] G. Mugala, R. Eriksson: "High frequency characteristics of a shielded medium voltage XLPE cable", *Annual Report Conference on Electrical Insulation and Dielectric Phenomena,* 2001, pp. 132-136.

[9] M. Popov, R.P.P. Smeets, L. van der Sluis, H. de Herdt, J. Declercq, "Experimental and Theoretical Analysis of Vacuum Circuit Breaker Prestrike Effect on a Transformer", *IEEE Trans. Power Delivery,* July 2009